Long-wavelength visible to near infrared photoluminescence from carbon-bridged styrylstilbene and thiadiazole conjugates in organic and aqueous media†

Takeru Inoue,[a] Makoto Tsurui,[b] Hiroshi Yamagishi, [iD][c] Yuma Nakazawa,[a] Naoto Hamaguchi,[a] Shoya Watanabe,[a] Yuichi Kitagawa, [iD][b] Yasuchika Hasegawa, [iD][b] Yohei Yamamoto [iD][c] and Hayato Tsuji [iD] *[a]

Donor–acceptor–donor conjugates composed of electron-donating carbon-bridged styrylstilbene (COPV2) and electron-accepting thiadiazole derivatives equipped with carbazolyl (Cz) terminators, **Cz-COPV2-A-COPV2-Cz** (A = benzothiadiazole (**BTz**), naphthobis(thiadiazole) (**NTz**), or benzobis(thiadiazole) (**BBTz**)), were newly synthesized and found to serve as efficient and stable long-wavelength photoluminescent dyes in organic and aqueous media. In particular, **Cz-COPV2-BBTz-COPV2-Cz** showed photoluminescence in the near infrared region (895–927 nm) with a photoluminescence quantum yield (PLQY) of up to 0.19 in cyclohexane and of 0.02–0.03 in THF/water mixtures. Its analogues with weaker acceptors, **Cz-COPV2-BTz-COPV2-Cz** and **Cz-COPV2-NTz-COPV2-Cz**, showed yellow to deep-red emission in organic solvents, with PLQYs of up to 0.71 in organic solvents and 0.45 in THF/water mixtures.

Introduction

Long-wavelength visible to near-infrared (NIR) light-emitting materials have found a broad range of applications, in *e.g.* sensors, electroluminescence, telecommunications, and bio-imaging.[1–5] Organic NIR-emitting dyes have attracted increasing attention due to the tunability of their emission wavelength *via* molecular design, the absence of rare and/or toxic metals in their structures, and their biocompatibility, although their luminescence efficiency still requires further improvement. To achieve long-wavelength emission using such dyes, extending the π-conjugated skeleton and connecting electron-donating and -accepting groups is widely used as a design principle.[1] However, the resulting molecules often suffer from disadvantages such as conformational disorder arising from free rotation around single bonds within the extended π-conjugated skeleton and strong intermolecular interactions that can cause

aggregation, which often results in low emission efficiency by aggregation-caused quenching (ACQ).

To circumvent the conformational disorder and reduce undesirable molecular motions, physical approach has been adopted in such ways as fixing molecular structures in low-temperature matrices for a long time, and more recently, aggregation-induced emission (AIE)[6–8] and albumin-induced emission.[9–13] Chemical construction of the structurally fixed molecules in terms of ladder-type structures that are rigidly planarized by sp³-carbon bridges[14,15] and that contain bulky substituents would be an alternative methodology. To this end, we have developed carbon-bridged oligo(*p*-phenylenevinylene) (COPV),[16–18] which features a rigid planar phenylenevinylene skeleton with bulky substituents on the bridging carbon atoms. The strong emission of COPVs in the visible region and their utility as active materials in organic lasers have been demonstrated.[19–26] These compounds also exhibit relatively high HOMO energy levels, which make them suitable as energy donors.[27,28] Herein, we report conjugates of carbon-bridged styrylstilbene (COPV2) and benzo- or naphtho-fused thiadiazole[29–31] (Fig. 1) that exhibit efficient long-wavelength emission with photoluminescence quantum yields (PLQYs) of up to 0.71 in the visible and 0.19 in the NIR regions.

Results and discussion

This desirable molecular structure was designed based on the time-dependent density functional theory (TD DFT) calculations

[a]Department of Chemistry, Faculty of Science, Kanagawa University, Tsuchiya 2946, Hiratsuka 259-1293, Japan. E-mail: tsujiha@kanagawa-u.ac.jp

[b]Faculty of Engineering, Hokkaido University, Kita13 Nishi8, Kita-ku, Sapporo 060-8628, Japan

[c]Department of Materials Science, Faculty of Pure and Applied Sciences, Tsukuba Research Center for Energy Materials Science (TREMS), University of Tsukuba, 1-1-1 Tennodai, Tsukuba, Ibaraki 305-8573, Japan

† Electronic supplementary information (ESI) available. See DOI: 10.1039/d0ra10201f
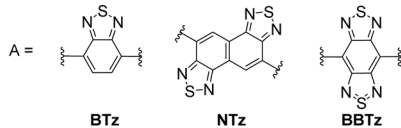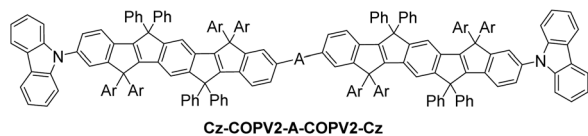
Fig. 1 Molecular structure of **Cz-COPV2-A-COPV2-Cz** (A = BTz, NTz, and BBTz; Ar = *p*-octylphenyl group).

of several model compounds at the CAM-B3LYP/6-31G* level of theory using **COPV2′** (a model compound without aromatic substituents on the sp³-hybridized carbon atoms in the bicyclo [2.2.0]octene moieties to reduce calculation cost) and benzothiadiazole (**BTz**) as the donor and acceptor, respectively (Fig. S1 and Table S1†). The donor–acceptor (D–A) diad **COPV2′-BTz** and the triads **BTz-COPV2′-BTz** (A–D–A) and **COPV2′-BTz-COPV2′** (D–A–D) were examined first. Among these architectures, the D–A–D triad **COPV2′-BTz-COPV2′** was expected to show the longest absorption wavelength and the largest transition oscillator strengths for both absorption and emission. The installation of carbazole terminators into this compound[32–35] to afford **Cz-COPV2′-BTz-COPV2′-Cz** with a D¹–D²–A–D²–D¹ architecture was expected to result in only a slight shift in the absorption and emission wavelengths but a significant increase in the transition oscillator strengths. Thus, a series of compounds with the carbazole-terminated architecture **Cz-COPV2-A-COPV2-Cz** was synthesized using **BTz** or the more electron-accepting naphthobis(thiadiazole) (**NTz**) or benzobis(thiadiazole) (**BBTz**) moieties as the acceptor (A).

The designed dyes were prepared *via* cross-coupling reactions as shown in Scheme 1. A Suzuki–Miyaura reaction

between **Cz-COPV2-Br** and either bis(pinacolatoboryl)benzothiadiazole (**BTz-(Bpin)₂**) or bis(pinacolatoboryl)naphthobis(thiadiazole) (**NTz-(Bpin)₂**) afforded **Cz-COPV2-BTz-COPV2-Cz** and **Cz-COPV2-NTz-COPV2-Cz** in 90 and 85% yield, respectively.[36] A Kosugi–Migita–Stille coupling between **Cz-COPV2-SnMe₃** and dibromobenzobis(thiadiazole) (**Br-BBTz-Br**)[37–43] was suitable for the preparation of **Cz-COPV2-BBTz-COPV2-Cz**. The structures of the products were characterized using ¹H and ¹³C NMR spectroscopy as well as mass spectrometry (for details, see the ESI†).

The absorption and emission spectra in cyclohexane, THF, chloroform, and THF/water mixtures are shown in Fig. 2, and the corresponding numerical data are summarized in Table 1. **Cz-COPV2-A-COPV2-Cz** showed two distinct absorption bands (solid lines in Fig. 2). The shorter wavelength one at 406–442 nm with a vibronic fine structure was less sensitive to the acceptor than the other broad band, which exhibited significant bathochromic shifts depending on the electron-withdrawing ability of the acceptor group (**Cz-COPV2-BTz-COPV2-Cz**: 469 nm; **Cz-COPV2-BBTz-COPV2-Cz**: 730 nm). As suggested by calculations (*vide infra*), the former band was assigned to the transition to an excited state localized in the COPV2 moiety (LE band), while the latter was attributed to the lowest excited state with charge-transfer character from the COPV2 moieties to the acceptor (CT band, see also $E_T(30)$ plot[44] in Fig. S2†).

Excitation at the CT band in the organic solvents afforded photoluminescence with a yellow-orange color for **Cz-COPV2-BTz-COPV2-Cz** (569–619 nm) and orange-red color for **Cz-COPV2-NTz-COPV2-Cz** (590–668 nm), depending on the solvent polarity. The photoluminescence quantum yields (PLQYs) for the CT emission were 0.60–0.71, and their fluorescence lifetimes and decay constants were typical values for fluorescence from organic compounds. The emission band of **Cz-COPV2-BBTz-COPV2-Cz**, which contained a strongly electron-withdrawing benzobis(thiadiazole) moiety, appeared in the
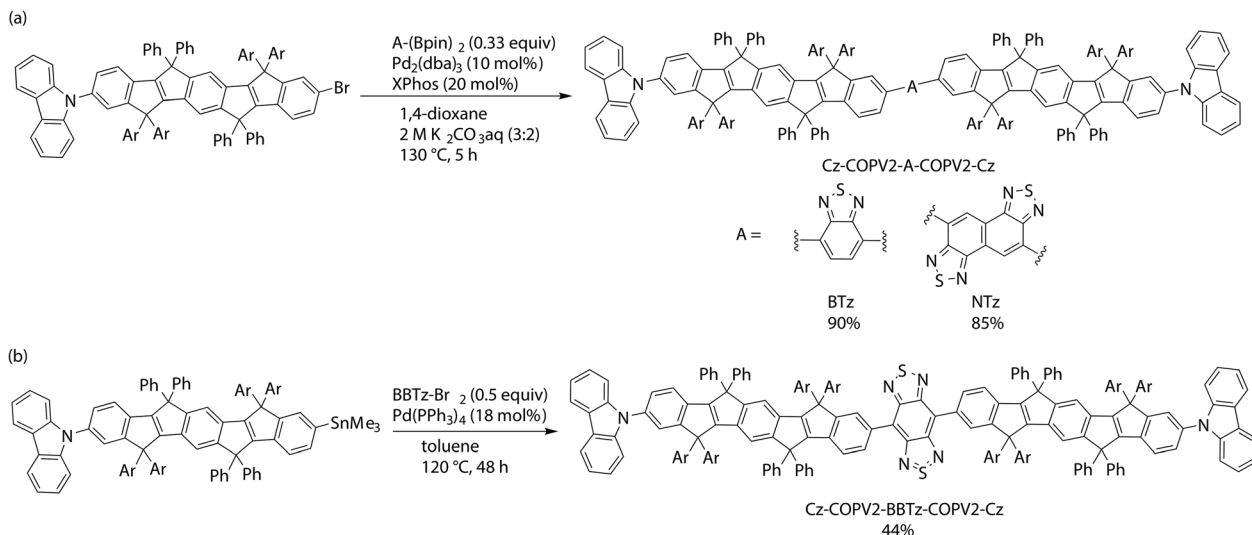
Scheme 1 (a) Synthesis of **Cz-COPV2-A-COPV2-Cz** (A = BTz or NTz) by Suzuki–Miyaura coupling and (b) **Cz-COPV2-BBTz-COPV2-Cz** by Kosugi–Migita–Stille coupling.
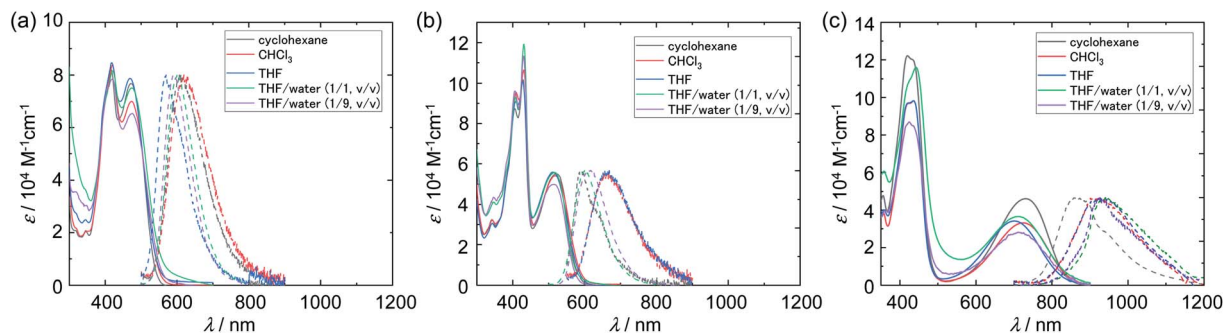
Fig. 2 Absorption spectra (solid lines) and photoluminescence spectra (dashed lines) of **Cz-COPV2-A-COPV2-Cz** in different solvents; (a) A = **BTz**, (b) A = **NTz**, (c) A = **BBTz**.

NIR region (750–1200 nm). In cyclohexane, the emission peak was observed at 895 nm (PLQY: 0.19), which is relatively high for NIR emission[4,45,46] and much higher than those of previously reported quinoidal COPV derivatives.[47,48] The emission peak was further bathochromically shifted to 927 and 925 nm in the polar organic solvents THF and chloroform, with decreased PLQYs of 0.04 and 0.06, respectively. The fluorescence quenching in these polar solvents was also obvious in the lifetime measurements and calculated non-radiative decay constants, which obeyed the low-bandgap law.[49]

THF/water solutions were prepared by adding water to the THF solutions of the dyes. The resulting solutions of **Cz-COPV2-BTz-COPV2-Cz** and **Cz-COPV2-BBTz-COPV2-Cz** appeared to be homogeneous at micromolar concentrations and showed photoluminescence similar to that in organic solvents with a slight spectral shift. The emission peak of **Cz-COPV2-BTz-COPV2-Cz** was slightly hypsochromically shifted compared to that in THF [THF: 607 nm; THF/water (1/1, v/v): 600 nm; THF/water (1/9, v/v): 593 nm], and the PLQYs were moderate [THF/water (1/1, v/v): 0.45; THF/water (1/9, v/v): 0.37], with a single exponential

decay profile in the fluorescence lifetime measurements. In contrast, the 'fresh' solution (immediately after preparation) of **Cz-COPV2-NTz-COPV2-Cz** in THF/water (1/1, v/v) also appeared to be homogeneous, but formed visible precipitates after 12 hours. The emission maxima of the fresh solution of **Cz-COPV2-NTz-COPV2-Cz** in THF/water showed hypsochromic shifts of up to 64 nm [THF/water (1/1, v/v): 600 nm; THF/water (1/9, v/v): 613 nm] relative to that in THF (664 nm). These emission maxima are similar to that in nonpolar cyclohexane (590 nm), and the fluorescence decay profile became biexponential, accompanying a short-lifetime component. These results suggest that **Cz-COPV2-NTz-COPV2-Cz** forms aggregates in aqueous media and that their local environment is rather hydrophobic and nonpolar,[50,51] which seems to be a plausible origin of the drastic hypsochromic shift of the spectrum.

TD DFT calculations of model compounds at the CAM-B3LYP/6-31G* level supported the assignments of the spectral data (Table S2, Fig. S3 and S4†). The CT absorption at longer wavelength was assigned to the transition to the lowest excited state (S₁), i.e., the HOMO → LUMO transition, where HOMO is

Table 1 Summary of the photophysical properties

| A | Solvent | λ_{abs}/nm | Photoluminescence | | | | |
			λ^a/nm	$\Phi^{a,b}$	τ^c/ns	$k_r^d/10^8$ s^{-1}	$k_{nr}^d/10^8$ s^{-1}
BTz	Cyclohexane	416, 469	569	0.71	2.26	3.14	1.28
	CHCl$_3$	420, 473	619	0.65	3.23	2.01	1.08
	THF	418, 469	607	0.70	3.02	2.32	0.99
	THF/water (1/1, v/v)	421, 475	600	0.45	2.22	2.03	2.48
	THF/water (1/9, v/v)	419, 475	593	0.37	2.05	1.80	3.07
NTz	Cyclohexane	406, 428, 522	590	0.71	2.60	2.73	1.12
	CHCl$_3$	409, 430, 518	668	0.60	3.89	1.54	1.03
	THF	408, 428, 512	664	0.60	3.76	1.60	1.06
	THF/water (1/1, v/v)	408, 516	600	0.42	1.10 (0.72), 2.72 (0.28)	—	—
	THF/water (1/9, v/v)	406, 514	613	0.25	0.54 (0.79), 1.80 (0.21)	—	—
BBTz	Cyclohexane	420, 730	895	0.19^e	1.29	1.47	6.28
	CHCl$_3$	436, 725	925	0.06^e	0.49	1.22	19.2
	THF	436, 702	927	0.04^e	0.35	1.14	27.4
	THF/water (1/1, v/v)	442, 715	949	0.02^e	0.40	0.55	24.4
	THF/water (1/9, v/v)	424, 710	944	0.03^e	0.80	0.38	12.1

^{a} Excited at each peak of the CT band. ^{b} The photoluminescence quantum yield was determined by the absolute method for the **BTz** and **NTz** derivatives, and by the relative method for the **BBTz** derivatives. ^{c} Fluorescence lifetime with excitation using a 470 nm LED for **BTz** and **NTz**, and a 630 nm LED for **BBTz**. ^{d} Radiative decay constant (k_r) and non-radiative decay constant (k_{nr}) calculated from Φ and τ. ^{e} Quantum yields were obtained using indocyanine green (ICG) in dimethylsulfoxide ($\Phi = 0.13$) as a standard.[52]

composed of two COPV2′ parts and the connecting phenylene or naphthylene moiety, and LUMO is localized within the arylenethiadiazole part. Significant redshift of the BBTz-derivative is well understood in terms of lowering the LUMO energy level (−2.38 eV for **BBTz** vs. −1.22 eV for **BTz**) based on the strong electron-accepting nature of the **BBTz** group. Calculations on the emission wavelengths were also performed using the optimized S_1 geometry. They reproduced the experimental data well (552 nm for **BTz**, 568 nm for **NTz**, and 907 nm for **BBTz**) and suggests that these molecules obey Kasha's rule. The LE absorption at shorter wavelength is attributed to the transition to the S_3 state for **Cz-COPV2′-BTz-COPV2′-Cz** and **Cz-COPV2′-NTz-COPV2′-Cz** or the S_4 state for **Cz-COPV2′-BBTz-COPV2′-Cz**. There are significant contributions of the orbitals localized in the COPV2′ parts, such as HOMO−1 and LUMO+1/LUMO+2 (for **BTz** and **BBTz**) or LUMO+2/LUMO+3 (for **NTz**), whose orbital energy levels are rather insensitive to the acceptor part. More detailed insight into the S_1 and S_3 states was obtained by the geometry optimization of the excited states of **Cz-COPV2′-BTz-COPV2′-Cz** (Table S3†). In the S_1 state, the bond lengths in the **BTz** unit (r_{11}) and those adjacent to the **BTz** unit (r_8 and r_{10}) changed drastically, and the dihedral angle between **BTz** and COPV2 became much smaller than in the ground state (ω_2: 38.48° at S_0; 17.40° at S_1). In the S_3 state, the COPV unit exhibited significant structural change, whereas little change was observed in the **BTz** unit, suggesting an LE character of the excited state. Specifically, the bond lengths in the COPV2 unit of the excited state showed quinoidal bond alternation similar to that observed in the first excited state of the parent COPV2.

Experimental

Synthetic procedures

Cz-COPV2-BTz-COPV2-Cz. A mixture of **Cz-COPV2-Br** (100 mg, 61.3 μmol), 4,7-bis(4,4,5,5-tetramethyl-1,3,2-dioxaborolan-2-yl)-2,1,3-benzothiadiazole (7.8 mg, 20 μmol), $Pd_2(dba)_3$ (5.9 mg, 6.4 μmol), and XPhos (6.5 mg, 14 μmol) in 1,4-dioxane (1.1 mL) and 2 M K_2CO_3aq (0.7 mL) was stirred at 130 °C for 5 h under argon atmosphere. After cooling to room temperature, the reaction mixture was diluted with chloroform and passed through a short plug of silica gel. The solvent was removed under reduced pressure. The residue was purified on silica-gel column chromatography (hexane/chloroform = 3/1) to afford **Cz-COPV2-BTz-COPV2-Cz** (57.7 mg, 85% yield) as an orange solid. ^{1}H NMR (600 MHz, CDCl$_3$): δ 0.85–0.89 (m, 24H), 1.26–1.33 (m, 80H), 1.52–1.56 (m, 16H), 2.49–2.52 (m, 16H), 6.95–6.98 (m, 16H), 7.16–7.37 (m, 78H), 7.55 (s, 2H), 7.63 (d, J = 1.4 Hz, 2H), 7.81 (dd, J = 7.9 and J = 1.7 Hz, 2H), 7.91 (d, J = 1.4 Hz, 2H), 8.08 (d, J = 7.6 Hz, 4H); ^{13}C NMR (150 MHz, CDCl$_3$): δ 14.2, 22.8, 29.4, 29.6, 29.6, 29.7, 31.4, 31.5, 32.0, 35.7, 35.7, 62.7, 63.1, 63.1, 76.9, 77.1, 77.3, 110.1, 118.2, 118.3, 119.9, 120.3, 120.6, 121.2, 123.4, 123.8, 125.3, 125.9, 126.8, 126.9, 127.9, 128.3, 128.4, 128.4, 128.5, 128.5, 128.8, 133.2, 134.7, 134.9, 136.6, 136.8, 137.8, 139.1, 139.8, 140.1, 140.7, 141.5, 141.7, 143.4, 143.5, 153.8, 154.1, 154.3, 156.4, 156.6, 157.1, 157.1, 157.8, 159.2. MS (MALDI-TOF): 3236.56 [M]$^{+}$.

Cz-COPV2-NTz-COPV2-Cz. 90% yield. ^{1}H NMR (400 MHz, CDCl$_3$): δ 0.84–0.88 (m, 24H), 1.24–1.36 (m, 80H), 1.51–1.59 (m, 16H), 2.52 (t, J = 7.3 Hz, 16H), 6.97–7.01 (m, 16H), 7.17 (d, J = 8.2 Hz, 8H), 7.21–7.38 (m, 70H), 7.64 (s, 2H), 7.93 (d, J = 9.2 Hz, 2H), 8.08 (d, J = 7.8 Hz, 4H), 8.18 (s, 2H), 8.85 (s, 2H); ^{13}C NMR (150 MHz, CDCl$_3$): δ 14.2, 22.8, 29.4, 29.6, 29.6, 29.7, 31.4, 31.5, 32.0, 35.7, 35.7, 62.7, 62.9, 63.1, 63.1, 76.9, 77.1, 77.3, 110.1, 118.2, 118.4, 119.9, 120.3, 120.7, 121.2, 123.4, 123.8, 125.0, 125.2, 125.3, 125.9, 126.1, 126.9, 126.9, 128.3, 128.4, 128.5, 128.8, 133.9, 134.2, 134.9, 136.7, 136.8, 137.8, 139.7, 139.8, 140.0, 140.7, 141.6, 141.7, 143.4, 143.5, 153.8, 153.9, 154.0, 154.2, 156.4, 156.7, 157.1, 157.6, 157.9, 159.2. MS (MALDI-TOF): 3346.67 [M]$^{+}$.

Cz-COPV2-BBTz-COPV2-Cz. A mixture of **Cz-COPV2-SnMe$_3$** (10.6 mg, 6.18 μmol), 4,7-dibromobenzo[1,2-c:4,5-c′]bis([1,2,5]thiadiazole) (1.1 mg, 3.1 μmol) and Pd(PPh$_3$)$_4$ (1.3 mg, 1.1 μmol) in toluene (1.0 mL) was stirred at 120 °C for 48 h under argon atmosphere. After cooling to room temperature, the reaction mixture was diluted with chloroform and passed through a short plug of silica gel. The solvent was removed under reduced pressure. The residue was purified on silica-gel column chromatography (hexane/chloroform = 3/1), and purified further with preparative GPC (eluent: chloroform) to afford **Cz-COPV2-BBTz-COPV2-Cz** (4.5 mg, 44% yield) as a green solid. ^{1}H NMR (400 MHz, CDCl$_3$): δ 0.84–0.88 (m, 24H), 1.24–1.33 (m, 80H), 1.51–1.58 (m, 16H), 2.48–2.53 (m, 16H), 6.96–6.99 (m, 16H), 7.17 (d, J = 8.2 Hz, 8H), 7.21–7.35 (m, H), 7.38–7.39 (m, 4H), 7.41 (s, 4H), 7.64 (s, 2H), 8.02 (dd, J = 8.0 and 1.6 Hz, 2H), 8.08 (d, J = 7.8 Hz, 4H), 8.34 (d, J = 1.8 Hz, 2H); ^{13}C NMR (150 MHz, CDCl$_3$): δ 14.2, 22.8, 29.3, 29.6, 29.6, 29.7, 31.4, 31.4, 32.0, 35.7, 35.7, 62.7, 62.8, 63.1, 63.1, 76.9, 77.1, 77.3, 110.1, 118.2, 118.4, 119.9, 120.3, 120.5, 121.2, 121.3, 123.4, 123.8, 125.3, 125.9, 126.9, 126.9, 128.3, 128.3, 128.4, 128.5, 128.6, 128.8, 128.8, 129.1, 130.9, 132.3, 134.9, 136.7, 136.9, 137.8, 139.6, 139.8, 140.0, 140.7, 141.5, 141.7, 143.4, 143.4, 152.8, 153.9, 154.4, 156.4, 156.8, 157.1, 157.2, 157.9, 159.2. MS (MALDI-TOF): 3295.89 [M]$^{+}$.

Spectroscopy

UV/vis absorption spectra were measured on JASCO V-670 or JASCO V-770. Fluorescence spectra were measured on JASCO FP-6500 for UV/vis region and a Horiba/Jobin-Yvon Fluorolog-3 spectrofluorometer equipped with a Hamamatsu R5509-43 photomultiplier for detecting NIR emissions using optical filters (excitation: SIGMAKOKI SCF-50S-58O, emission: SIGMAKOKI SCF-50S-60R) to remove higher-order diffraction of ultraviolet or visible light. Photoluminescence quantum yields for ultraviolet and visible region were measured on Hamamatsu Photonics C9920-02 Absolute PL Quantum Yield Measurement System, and absolute quantum yields were determined by using a calibrated integrating sphere system. The quantum yields in NIR region were obtained based on ICG in dimethylsulfoxide (Φ = 0.13) as a standard. Fluorescence lifetimes were estimated with the time correlated single photon counting (TCSPC) operation mode on Hamamatsu Photonics C11367-02.

Calculations

Geometry optimization of the ground state of each compound was performed at the CAM-B3LYP/6-31G* level using Gaussian 09.[53] Calculations of the excitation energy and oscillator strength, along with the geometry optimization of the excited states were performed using time-dependent (TD) DFT calculations at the CAM-B3LYP/6-31G* level.

Conclusions

In summary, the efficacy of the use of the rigid planar electron-donating carbon-bridged styrylstilbene moiety (COPV2) to achieve efficient long-wavelength emission especially in NIR region was demonstrated in COPV2–thiadiazole conjugates. A noteworthy feature of the present chemical fixation method by intramolecular bridging is that once synthesized, the rigidity of the molecular structure is maintained even in room temperature solution independent of the solvent and without additives. The present work demonstrates that this feature played a key role in the NIR emission, which otherwise often results in low efficiency due to undesired structural disorder and molecular motion. The application of these dyes to optical devices and attempts to further elongate the spectral bathochromic shift *via* the use of longer COPV homologues and other types of acceptors are also currently under investigation in our groups, and the results will be reported in due course.

Conflicts of interest

There are no conflicts to declare.

Acknowledgements

Notes and references

1 G. Qian and Z. Y. Wang, *Chem.–Asian J.*, 2010, **5**, 1006–1029.

2 H. Zhu, J. Fan, J. Du and X. Peng, *Acc. Chem. Res.*, 2016, **49**, 2115–2126.

3 J. Qi, W. Qiao and Z. Y. Wang, *Chem. Rec.*, 2016, **16**, 1531–1548.

4 A. Zampetti, A. Minotto and F. Cacialli, *Adv. Funct. Mater.*, 2019, **29**, 1807623.

5 C. Li, G. Chen, Y. Zhang, F. Wu and Q. Wang, *J. Am. Chem. Soc.*, 2020, **142**, 14789–14804.

6 J. Luo, Z. Xie, J. W. Y. Lam, L. Cheng, H. Chen, C. Qiu, H. S. Kwok, X. Zhan, Y. Liu, D. Zhu and B. Z. Tang, *Chem. Commun.*, 2001, 1740–1741.

7 Y. Hong, J. W. Y. Lama and B. Z. Tang, *Chem. Commun.*, 2009, 4332–4353.

8 S. Suzuki, S. Sasaki, A. S. Sairi, R. Iwai, B. Z. Tang and G.-i. Konishi, *Angew. Chem., Int. Ed.*, 2020, **59**, 9856–9867.

9 Y. Hong, C. Feng, Y. Yu, J. Liu, J. W. Y. Lam, K. Q. Luo and B. Z. Tang, *Anal. Chem.*, 2010, **82**, 7035–7043.

10 X. Xu, J. Huang, J. Li, J. Yan, J. Qin and Z. Li, *Chem. Commun.*, 2011, **47**, 12385–12387.

11 W. Li, D. Chen, H. Wang, S. Luo, L. Dong, Y. Zhang, J. Shi, B. Tong and Y. Dong, *ACS Appl. Mater. Interfaces*, 2015, **7**, 26094–26100.

12 S. I. Reja, I. A. Khan, V. Bhalla and M. Kumar, *Chem. Commun.*, 2016, **52**, 1182–1185.

13 R. Tian, Q. Zeng, S. Zhu, J. Lau, S. Chandra, R. Ertsey, K. S. Hettie, T. Teraphongphom, Z. Hu, G. Niu, D. O. Kiesewetter, H. Sun, X. Zhang, A. L. Antaris, B. R. Brooks and X. Chen, *Sci. Adv.*, 2019, **5**, eaaw0672.

14 U. Scherf, *J. Mater. Chem.*, 1999, **9**, 1853–1864.

15 A. C. Grimsdale and K. Müllen, *Macromol. Rapid Commun.*, 2007, **28**, 1676–1702.

16 H. Tsuji and E. Nakamura, *Acc. Chem. Res.*, 2019, **52**, 2939–2949.

17 X. Zhu, C. Mitsui, H. Tsuji and E. Nakamura, *J. Am. Chem. Soc.*, 2009, **131**, 13596–13597.

18 X. Zhu, H. Tsuji, J. T. López Navarrete, J. Casado and E. Nakamura, *J. Am. Chem. Soc.*, 2012, **134**, 19254–19259.

19 M. Morales-Vidal, P. G. Boj, J. M. Villalvilla, J. A. Quintana, Q. Yan, N.-T. Lin, X. Zhu, N. Ruangsupapichat, J. Casado, H. Tsuji, E. Nakamura and M. A. Díaz-García, *Nat. Commun.*, 2015, **6**, 8458.

20 P. M. Burrezo, N.-T. Lin, K. Nakabayashi, S.-i. Ohkoshi, E. M. Calzado, P. G. Boj, M. A. Díaz-García, C. Franco, C. Rovira, J. Veciana, M. Moos, C. Lambert, J. T. López Navarrete, H. Tsuji, E. Nakamura and J. Casado, *Angew. Chem., Int. Ed.*, 2017, **56**, 2898–2902.

21 J. A. Quintana, J. M. Villalvilla, M. Morales-Vidal, P. G. Boj, X. Zhu, N. Ruangsupapichat, H. Tsuji, E. Nakamura and M. A. Díaz-García, *Adv. Opt. Mater.*, 2017, **5**, 1700238.

22 M. Morales-Vidal, J. A. Quintana, J. M. Villalvilla, P. G. Boj, H. Nishioka, H. Tsuji, E. Nakamura, G. L. Whitworth, G. A. Turnbull, I. D. W. Samuel and M. A. Díaz-García, *Adv. Opt. Mater.*, 2018, **6**, 1800069.

23 V. Bonal, M. Morales-Vidal, P. G. Boj, J. M. Villalvilla, J. A. Quintana, N. Lin, S. Watanabe, H. Tsuji, E. Nakamura and M. A. Díaz-García, *Bull. Chem. Soc. Jpn.*, 2020, **93**, 751–758.

24 V. Bonal, J. M. Villalvilla, J. A. Quintana, P. G. Boj, N. Lin, S. Watanabe, K. Kazlauskas, O. Adomeniene, S. Jursenas, H. Tsuji, E. Nakamura and M. A. Díaz-García, *Adv. Opt. Mater.*, 2020, **8**, 2001153.

25 D. Okada, S. Azzini, H. Nishioka, A. Ichimura, H. Tsuji, E. Nakamura, F. Sasaki, C. Genet, T. W. Ebbesen and Y. Yamamoto, *Nano Lett.*, 2018, **18**, 4396–4402.

26 K. Iwai, H. Yamagishi, C. Herzberger, Y. Sato, H. Tsuji, K. Albrecht, K. Yamamoto, F. Sasaki, H. Sato, A. Asaithambi, A. Lorke and Y. Yamamoto, *Angew. Chem., Int. Ed.*, 2020, **59**, 12674–12679.

27 J. Sukegawa, H. Tsuji and E. Nakamura, *Chem. Lett.*, 2014, **43**, 699–701.

28 H. Tsuji, A. Ichimura, M. Kudo, J. Sukegawa and E. Nakamura, *Chem.–Asian J.*, 2019, **14**, 1672–1675.

29 M. Wang, X. Hu, P. Liu, W. Li, X. Gong, F. Huang and Y. Cao, *J. Am. Chem. Soc.*, 2011, **133**, 9638–9641.

30 I. Osaka, M. Shimawaki, H. Mori, I. Doi, E. Miyazaki, T. Koganezawa and K. Takimiya, *J. Am. Chem. Soc.*, 2012, **134**, 3498–3507.

31 K. Kawashima, T. Fukuhara, Y. Suda, Y. Suzuki, T. Koganezawa, H. Yoshida, H. Ohkita, I. Osaka and K. Takimiya, *J. Am. Chem. Soc.*, 2016, **138**, 10265–10275.

32 H. Uoyama, K. Goushi, K. Shizu, H. Nomura and C. Adachi, *Nature*, 2012, **492**, 234–238.

33 K. Albrecht, K. Matsuoka, K. Fujita and K. Yamamoto, *Angew. Chem., Int. Ed.*, 2015, **54**, 5677–5682.

34 A. S. D. Sandanayaka, T. Matsushima, F. Bencheikh, S. Terakawa, W. J. Potscavage Jr, C. Qin, T. Fujihara, K. Goushi, J.-C. Ribierre and C. Adachi, *Appl. Phys. Express*, 2019, **12**, 061010.

35 P. Ledwon, *Org. Electron.*, 2019, **75**, 105422.

36 H. Nishioka, H. Tsuji and E. Nakamura, *Macromolecules*, 2018, **51**, 2961–2968.

37 G. Qian, B. Dai, M. Luo, D. Yu, J. Zhan, Z. Zhang, D. Ma and Z. Y. Wang, *Chem. Mater.*, 2008, **20**, 6208–6216.

38 G. Qian, Z. Zhong, M. Luo, D. Yu, Z. Zhang, Z. Y. Wang and D. Ma, *Adv. Mater.*, 2009, **21**, 111–116.

39 T. Kono, D. Kumaki, J.-i. Nishida, S. Tokito and Y. Yamashita, *Chem. Commun.*, 2010, **46**, 3265–3267.

40 J. Fan, J. D. Yuen, M. Wang, J. Seifter, J.-H. Seo, A. R. Mohebbi, D. Zakhidov, A. Heeger and F. Wudl, *Adv. Mater.*, 2012, **24**, 2186–2190.

41 Z. Sheng, B. Guo, D. Hu, S. Xu, W. Wu, W. H. Liew, K. Yao, J. Jiang, C. Liu, H. Zheng and B. Liu, *Adv. Mater.*, 2018, **30**, 1800766.

42 Q. Yang, Z. Hu, S. Zhu, R. Ma, H. Ma, Z. Ma, H. Wan, T. Zhu, Z. Jiang, W. Liu, L. Jiao, H. Sun, Y. Liang and H. Dai, *J. Am. Chem. Soc.*, 2018, **140**, 1715–1724.

43 S. Liu, X. Zhou, H. Zhang, H. Ou, J. W. Y. Lam, Y. Liu, L. Shi, D. Ding and B. Z. Tang, *J. Am. Chem. Soc.*, 2019, **141**, 5359–5368.

44 C. Reichardt, *Chem. Rev.*, 1994, **94**, 2319–2358.

45 X. Du, J. Qi, Z. Zhang, D. Ma and Z. Y. Wang, *Chem. Mater.*, 2012, **24**, 2178–2185.

46 U. Mayerhöffer, M. Gsänger, M. Stolte, B. Fimmel and F. Würthner, *Chem.–Eur. J.*, 2013, **19**, 218–232.

47 X. Zhu, H. Tsuji, K. Nakabayashi, S.-i. Ohkoshi and E. Nakamura, *J. Am. Chem. Soc.*, 2011, **133**, 16342–16345.

48 R. C. González-Cano, S. di Motta, X. Zhu, J. T. López Navarrete, H. Tsuji, E. Nakamura, F. Negri and J. Casado, *J. Phys. Chem. C*, 2017, **121**, 23141–23148.

49 R. Englman and J. Jortner, *Mol. Phys.*, 1970, **18**, 145–164.

50 T. Ishi-i, R. Hashimoto and M. Ogawa, *Asian J. Org. Chem.*, 2014, **3**, 1074–1082.

51 T. Ishi-i, K. Ikeda, M. Ogawa and Y. Kusakaki, *RSC Adv.*, 2015, **5**, 89171–89187.

52 K. Licha, B. Riefke, V. Ntziachristos, A. Becker, B. Chance and W. Semmler, *Photochem. Photobiol.*, 2000, **72**, 392–398.

53 M. J. Frisch, G. W. Trucks, H. B. Schlegel, G. E. Scuseria, M. A. Robb, J. R. Cheeseman, G. Scalmani, V. Barone, B. Mennucci, G. A. Petersson, H. Nakatsuji, M. Caricato, X. Li, H. P. Hratchian, A. F. Izmaylov, J. Bloino, G. Zheng, J. L. Sonnenberg, M. Hada, M. Ehara, K. Toyota, R. Fukuda, J. Hasegawa, M. Ishida, T. Nakajima, Y. Honda, O. Kitao, H. Nakai, T. Vreven, J. A. Montgomery Jr, J. E. Peralta, F. Ogliaro, M. Bearpark, J. J. Heyd, E. Brothers, K. N. Kudin, V. N. Staroverov, T. Keith, R. Kobayashi, J. Normand, K. Raghavachari, A. Rendell, J. C. Burant, S. S. Iyengar, J. Tomasi, M. Cossi, N. Rega, J. M. Millam, M. Klene, J. E. Knox, J. B. Cross, V. Bakken, C. Adamo, J. Jaramillo, R. Gomperts, R. E. Stratmann, O. Yazyev, A. J. Austin, R. Cammi, C. Pomelli, J. W. Ochterski, R. L. Martin, K. Morokuma, V. G. Zakrzewski, G. A. Voth, P. Salvador, J. J. Dannenberg, S. Dapprich, A. D. Daniels, O. Farkas, J. B. Foresman, J. V. Ortiz, J. Cioslowski, and D. J. Fox, *Gaussian 09, Revision E.01*, Gaussian, Inc., Wallingford CT, 2013.